STUDY OF BINARY $\pi^- p$ REACTIONS WITH NEUTRAL PARTICLES IN THE FINAL STATE AT THE PION CHANNEL OF THE PNPI SYNCHROCYCLOTRON

D.E. Bayadilov, Yu.A. Beloglazov, E.A. Filimonov, N.G. Kozlenko, S.P. Kruglov, I.V. Lopatin, D.V. Novinsky, A.K. Radkov, V.V. Sumachev

1. Introduction

During several years, the Meson Physics Laboratory performs at the pion channel of the PNPI synchrocyclotron a wide program of investigation pion-nucleon scattering in the region of low-lying πN resonances. At the first stages of this program, precision measurements of the differential cross sections, polarization parameters P and spin rotation parameters A and R were made for $\pi^{\pm} p$ elastic scattering at energies of incident pions in the range from 300 to 600 MeV (corresponding values of the incident pions momenta being from 417 to 725 MeV/c). In total, more than 400 new experimental points were obtained, which served – together with the results of experiments carried out at the Los-Alamos Meson Facility LAMRF – as a base of the new phase shift analysis PNPI-94. It became evidently in the course of performing this analysis that the mostly serious obstacle for determining phase shifts (and, consequently, partial amplitudes of πN scattering) with a higher precision is a lack of systematic data on $\pi^- p$ charge exchange scattering and η-production process. That is why the investigation of reactions $\pi^- p \to \pi^0 n$ and $\pi^- p \to \eta n$ has become a logical continuation of earlier experiments on the study of $\pi^{\pm} p$ elastic scattering.

For performing this new series of experiments, the Neutral Meson Spectrometer was designed and created at PNPI.

2. Neutral Meson Spectrometer

The main principle of the Neutral Meson Spectrometer (NMS) – determining the total energy of produced π^0 meson (η meson) E_{π° and the angle θ_{π° under which it produced on the base of measuring energies of two photons from the decay of π^0 meson (η meson) $E_{\gamma 1}$, $E_{\gamma 2}$ and angles of their emission $\theta_{\gamma 1}$, $\theta_{\gamma 2}$ (all values are in the lab. system):

$$E_{\pi^o} = \left[\frac{2M_{\pi^o}^2}{\left(1-\cos\Psi_{\gamma\gamma}\right)\cdot\left(1-X^2\right)} \right]^{1/2} , \qquad (1)$$

$X = (E_{\gamma 1} - E_{\gamma 2})/(E_{\gamma 1} + E_{\gamma 2})$ – the parameter which characterizes the sharing π^0 meson (η meson) energy among the two photons, $\Psi_{\gamma\gamma}$ – the angle between directions of emitted photons,

$$\cos\theta_{\pi^o} = \frac{E_{\gamma 1}\cos\theta_{\gamma 1} + E_{\gamma 2}\cos\theta_{\gamma 2}}{\left(E_{\gamma 1}^2 + E_{\gamma 2}^2 + 2E_{\gamma 1}E_{\gamma 2}\cos\Psi_{\gamma\gamma}\right)^{1/2}} . \qquad (2)$$

The schematic drawing of the NMS is shown in Fig. 1, the photo of its disposition at the experimental hall of PNPI synchrocyclotron is presented in Fig. 2. The NMS consists of two total absorption electromagnetic calorimeters, each being an array of 24 CsI(Na) crystals. The size of each crystal – $60 \times 60 \times 300$ mm^3; the last figure – thickness, it corresponds to 16.2 radiation lengths. Also shown (conditionally in Fig. 1) are a liquid hydrogen target and two veto counters intended for rejecting those events when a charged particle (but not a photon) enters the calorimeter.

For readout a pulse from each crystal, photomultiplier tubes (PMT) of type FEU-97 were used. For each of 48 PMTs a special stabilized high-voltage supplier was created the main principle of which is a voltage multiplication; each supplier was mounted directly on the PMT base. Signals from the output of each PMT were split – the anode signal was fed to a Charge-to-Digital Converter (CDC) and was used,

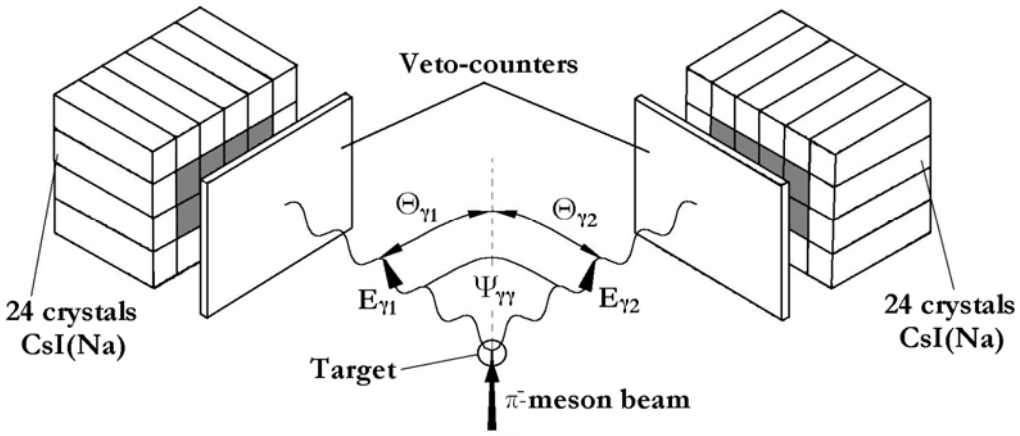

Fig. 1. Schematic drawing of the NMS

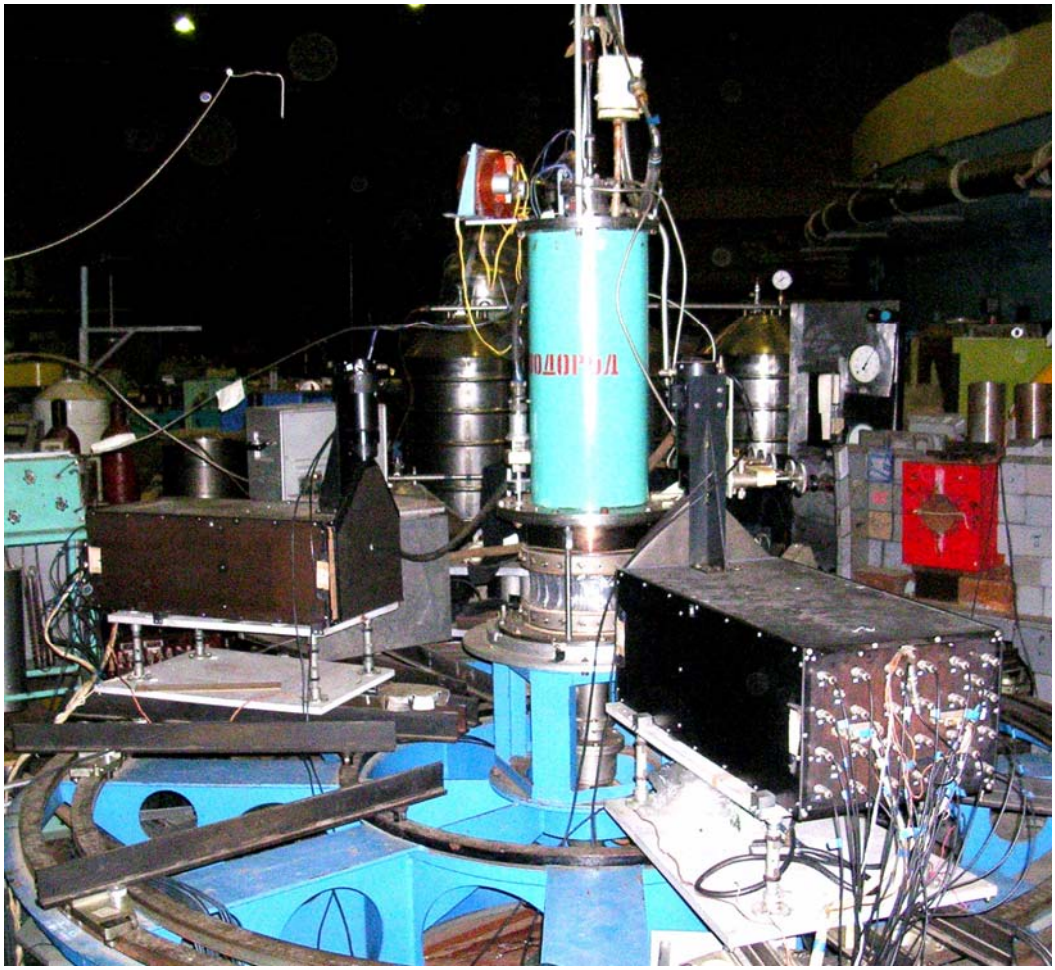

Fig. 2. General view of the experimental setup including the NMS and the liquid hydrogen target

consequently, for getting information about the energy deposited in the crystal, the signal from the last dynode was used for forming a fast trigger. In order to minimize an uncertainty in the determination of photon energy due a side leakage of the shower energy, the trigger was formed only in the case when energy deposited in eight inner crystals of each calorimeter exceeded some fixed value. For this purpose, dynode signals from 8 inner crystals were added up and after that the summed signal was fed to a shaper with the

threshold corresponding minimal required energy deposit. Surrounding 16 crystals played a role of somewhat like “guard ring” in which the shower energy carried out of central part of the calorimeter was registered.

The typical trigger to initiate a setup was formed as a coincidence of fast logical signals from the two calorimeters and from monitor counters provided there was no signal from veto counters placed in front of the calorimeters.

3. Energy calibration of spectrometer

In order from CDC readings one can determine the energy deposited in different crystals, it is necessary to perform the energy calibration of each chain crystal + PMT + CDC. In another words, it is necessary to find the dependence between the energy E_γ^i deposited in the crystal “*i*” and the number of corresponding CDC channel N_γ^i (after subtracting the pedestal which is located in the channel approximately 20). If this dependence is linear one (it will be shown below that it is actually so), E_γ и N_γ are connected by a simple proportion

$$E_\gamma^i = K^i N_\gamma^i, \tag{3}$$

and the task is to determine calibration coefficients K^i for all 48 chains crystal + PMT + CDC.

In principle, coefficient K^i can be determined by registering signals generated in the crystal due to the energy E_μ^i deposited by cosmic muons (*via* ionization losses) when traversing the crystal:

$$E_\mu^i = K^i N_\mu^i \ . \tag{4}$$

However, it is difficult to calculate the deposited energy E_μ^i with a high accuracy since the cosmic muons cross the crystal in different directions and their energy spectrum depends on the angle of incidence.

That is why for reliable determining the value E_μ^i a special experiment was carried out, in which several central crystals were irradiated by electrons; these electrons are available in the beam of negatively charged particles formed by the pion channel of the PNPI synchrocyclotron. To select electrons in the beam from pions we used a gas Cherenkov counter filled with CO_2 at 4 atm pressure; the counter was placed in the beam line just upstream of the liquid hydrogen target. During the calibration procedure, a narrow electron beam (defined by a small counter with the 2 cm diameter scintillator) was injected into the center of the crystal under investigation. The calibration was made at electron energies of 70, 120, 200, 300, 400, and 500 MeV. For each energy a position of a peak in the pulse height spectrum was determined. Because the lateral spreading of the electromagnetic shower a part of energy leaks from the injected crystal, so the energy deposited in this crystal is less than the energy of the incident electron. Corresponding correction was calculated using a Monte Carlo simulation, its value is about 15%. After introducing this correction, the positions of peaks in the pulse height spectra (measured in CDC channels) were plotted against the energy deposited in the crystal. Obtained dependence is described with a good accuracy by a straight line the slope of which determines the value of calibration coefficient K^i [1]. If we use now this dependence for determining the energy deposit corresponding to the number of CDC channel N_μ^i, we shall obtain $E_\mu^i = 36$ MeV. The similar result was obtained for all four central crystal irradiated by electrons.

Thus, the calibration coefficient is defined by the relation

$$K^i = 36 / N_\mu^i . \tag{5}$$

Just this coefficient K^i is used for determining the energy deposited in the crystal “*i*” in case when photon enters this crystal:

$$E_\gamma^i = K^i N_\gamma^i = (36 / N_\mu^i) \cdot N_\gamma^i . \tag{6}$$

---

[1] Since at rather high energies electromagnetic showers initiated by photons and by electrons develop in the matter almost identically, this coefficient may be considered equal to the coefficient K^i in the formula (3).

4. Measurements of differential cross sections of $\pi^- p$ charge exchange scattering at small angles

The first experiment [1–3] carried out using the NMS was aimed at measurements of differential cross sections of $\pi^- p$ charge exchange scattering $\pi^- p \to \pi^0 n$ at small angles. The measurements were made at ten momenta of incident pions in the range from 417 to 710 MeV/c (corresponding values of kinetic energy of pions – from 300 to 585 MeV); at each momentum the data acquisition was performed for both a hydrogen-filled and an empty target. A momentum distribution in the incident beam had the Gaussian form, the full width at half-maximum being 6%. The central value of the momentum was determined by readings of a Hall probe placed at the gap of the last bending magnet of the π-meson channel and was known with an accuracy of ±0.5%. The flux of pions incident on the target was about 10^5 1/s.

When carrying out the experiment, for each event energies and emission angles of two photons from the decay $\pi^0 \to \gamma\gamma$ were measured; after that the angle, at which π^0 meson was produced in the laboratory frame, could be determined using the relation (2). The main feature of the decay $\pi^0 \to \gamma\gamma$ is that it occurs with the most probability symmetrically in respect to the direction of π^0 meson. Since it was proposed in this experiment to detect only events with small scattering angles (*i. e.* small angles between the directions of produced π^0 mesons and incident pions), it is evidently that the two calorimeters of the NMS should be placed symmetrically (on the right and on the left) relatively to the beam axis. For the momenta of incident pions in the range from 417 to 710 MeV/c, π^0 mesons produced at small angles have the kinetic energy from 300 to 590 MeV, respectively; the angle between the two photons emitted symmetrically in respect to the direction of π^0 meson varies from 18° to 11°. Having this in mind and taking into account the size and construction of the NMS, we located the calorimeters at angles ±16° relatively to the beam axis; a distance from the center of the target to faces of the calorimeters was 101 cm.

To identify that in the considered event with two registered photons just π^0 meson was produced, the invariant mass of these two photons should be reconstructed; it must be equal to the rest mass of π^0 meson. The energies $E_{\gamma 1}$, $E_{\gamma 2}$ of both photons and the angle $\Psi_{\gamma\gamma}$ between them being known on the base equations (1) and (2), the invariant mass of the two photons can be calculated by formula:

$$M_{\gamma\gamma}^2 = 2E_{\gamma 1}E_{\gamma 2}(1-\cos\psi_{\gamma\gamma}). \qquad (7)$$

As an example, in Fig. 3 the distribution of events by the invariant mass of the two photons is shown for the momentum of the incident pions 614 MeV/c. A clear peak corresponding to the π^0 meson mass is seen.

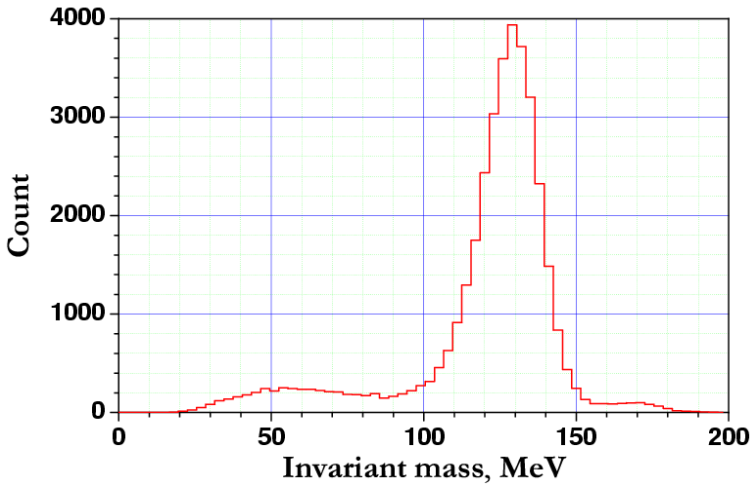

Fig. 3. Invariant $\gamma\gamma$-mass distribution for the incident pion momentum of 614 MeV/c

After the invariant mass is calculated, the next step of processing is the reconstruction of the missing mass. For the reaction $\pi^- p \to \pi^0 n$ it is the mass of the recoil neutron. For the analysis of accumulated data it is convenient to plot a two-dimensional distribution of events – the correlation between the missing mass and

the invariant mass; Fig. 4 illustrates a character of such distribution. Events caused by the charge exchange (CEX) reaction on the target's protons are concentrated in this Figure inside a dark spot of elliptical form. Also seen are background events due to the CEX reaction on nuclei of a monitor counter and of a mylar foil closing target's windows (points in the left upper part) as well as to the reaction of two π^0 production.

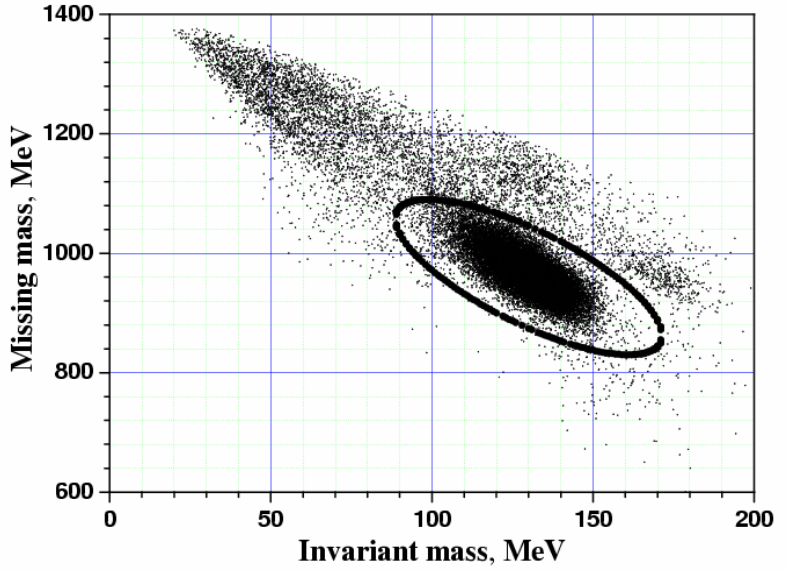

Fig. 4. Two-dimensional plot missing mass *vs* invariant mass for the incident pions momentum of 614 MeV/c

In further processing, only those events were considered "useful" (*i. e.* caused by the CEX reaction on protons of the target) which lay within the ellipse shown in Fig. 4. Using a Monte Carlo simulation, the correct shape and size of the ellipse were chosen so that 99% of all "useful" events were within this ellipse.

The "useful" events registered by the NMS cover the angular range from $\cos\theta^{cm}_{\pi^0}$=0.98 to $\cos\theta^{cm}_{\pi^0}$=1.00. To calculate differential cross sections, it is necessary to determine the angular distribution of these events. When plotting such distribution, the value of one angular bin was chosen to be equal $\Delta\cos\theta^{cm}_{\pi^0}$=0.002 taking into account the angular resolution of the NMS.

The differential cross section was calculated for each angular bin using the equation:

$$\frac{d\sigma^{cm}}{d\Omega} = \frac{N_{\pi^0}}{N_{\pi^-} \cdot A \cdot N_p \cdot 2\pi \cdot \Delta\cos\theta^{cm} \cdot BR(\pi^0 \to 2\gamma)}. \qquad (8)$$

Notations in this expression are as follows. N_{π^0} is the number of π^0 mesons produced in the reaction $\pi^- p \to \pi^0 n$, which are detected by the NMS during the experiment; N_{π^-} is the number of pions passed through the target in the course of the experiment; N_p is the number of protons in the target per cm^2; A is the angular acceptance obtained by a Monte Carlo simulation for the definite angular interval $\Delta\cos\theta^{cm}_{\pi^0}$; $2\pi \cdot \Delta\cos\theta^{cm}_{\pi^0}$ is the covered c.m.s. solid angle; $BR\ (\pi^0 \to 2\gamma)$ is the branching ratio of the decay $\pi^0 \to 2\gamma$ equal to (98.80 ± 0.03)%. It should be mentioned here that in the beam formed by the pion channel there exists also an admixture of muons and electrons, and an appropriate correction has to be introduced into the monitor counts when determining the number N_{π^-}.

As an example, the angular dependence of the differential cross section for the incident pions momentum of 614 MeV/c is presented in Fig. 5. One can see that the angular dependence is very weak in this range.

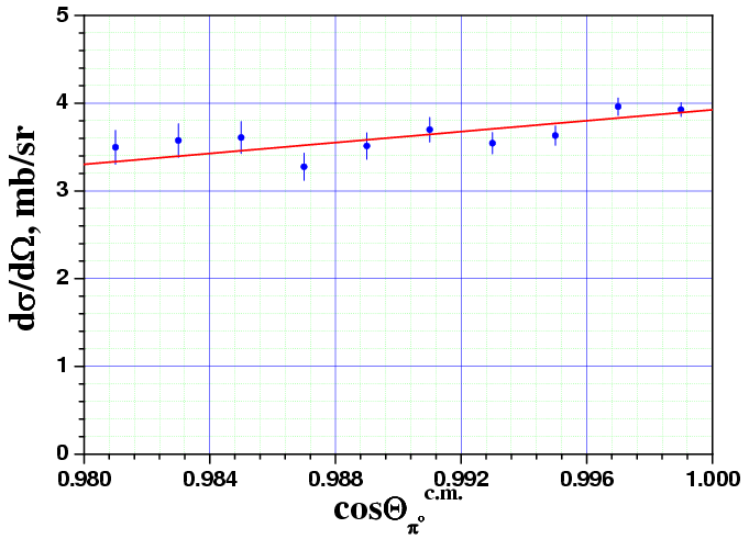

Fig. 5. Angular dependence of differential cross section for the incident pions momentum of 614 MeV/c

The value of differential cross section at zero degree was obtained by the extrapolation of this angular dependence to the point $\cos\theta_{\pi^0}^{cm}$=1.00. To do it, we used the least squares method in a linear approximation.

In Fig. 6 the obtained values $\frac{d\sigma}{d\Omega}(0^\circ)$ are plotted as a function of the incident pions momentum. Also shown are the results of previous experiments and the predictions of the partial-wave analyses (PWA) KH-80 (Karlsruhe-Helsinki) and SM-02 (the George Washington University, USA). One can see that our experiment is the mostly full and essentially more precision in the range of the incident pions momenta from 417 to 710 MeV/c. Experimental points obtained at PNPI have statistical uncertainties at a level of 2% exceeding significantly an accuracy of other experiments. The comparison with the predictions of different PWAs demonstrates that the new data obtained does not agree fully with the shown PWA predictions, although when comparing the momentum dependences some preference can be given to the PWA SM-02.

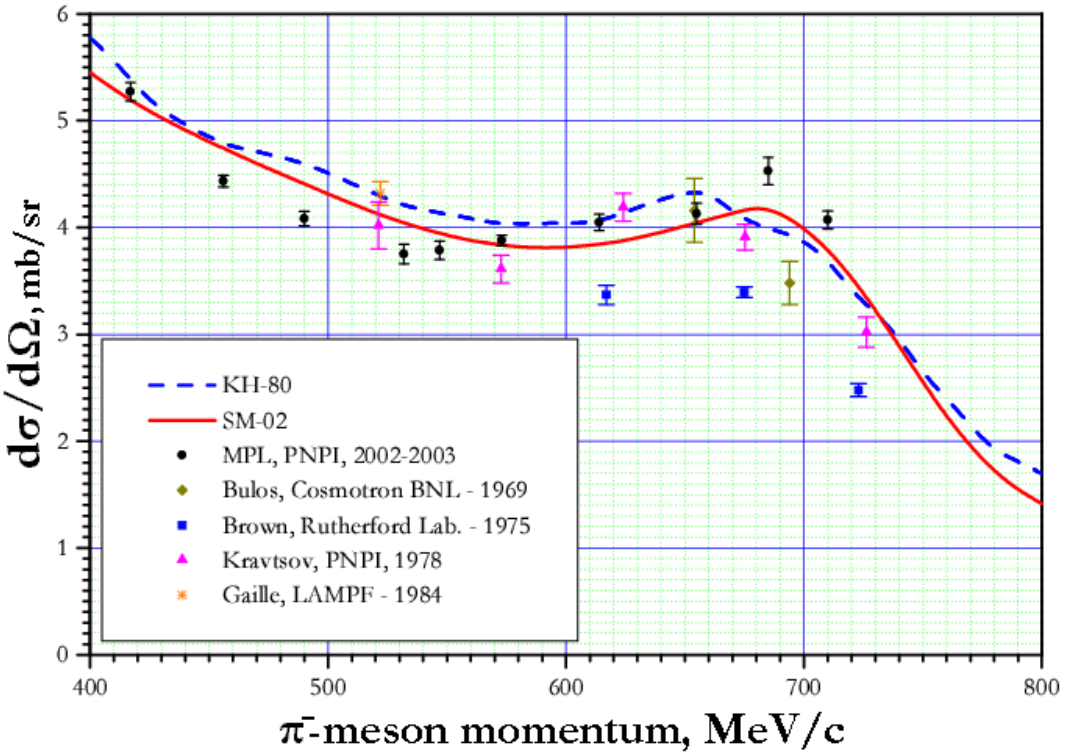

Fig. 6. Experimental results of this work (black circles) are given in comparison with data of previous experiments

5. Measurement of cross sections of the η-production process in the near-threshold region

In the next series of experiments, the NMS is used [4, 5] for measuring the cross section of the η-production in the reaction $\pi^- p \to \eta n$ at the incident pions momenta close to the threshold of this reaction (685 MeV/c). Since the cross section of this reaction rises sharply with the momentum in the near-threshold region, the momentum spread of particles in the beam was decreased down to 1.5% by putting a special vertical narrow beam slit in that part of the pion channel where the momentum dispersion is maximal.

The experimental layout was similar to that used for studying $\pi^- p$ charge exchange scattering at small angles, the main distinction – the calorimeters were placed at the distance 65 cm from the target center at the angles ±66° relatively to the pion beam axis – was dictated by the specific kinematics of the η-production process in the near-threshold region. The main peculiarity is that η mesons, which produced in the center-of-mass system in a wide angular range from $\theta_\eta^{cm} = 0°$ to $\theta_\eta^{cm} = 180°$, concentrate in a narrow angular cone after transferring to the laboratory system. So, at the incident pions momentum of 710 MeV/c the opening angle of this cone is ±23.5°. In the subsequent η-decay $\eta \to 2\gamma$, photons are emitted in the angular range from 0° to 180° (relatively to the momentum of the η meson), but their symmetrical emission ($\theta_{\gamma 1} \approx \theta_{\gamma 2}$) is mostly probable. These kinematical features allow to measure the differential cross sections of the reaction $\pi^- p \to \eta n$ in the full angular range from $\theta_\eta^{cm} = 0°$ to $\theta_\eta^{cm} = 180°$ using the NMS with a rather restricted angular acceptance.

In the course of the experiment on studying the reaction $\pi^- p \to \eta n$ the NMS detects in coincidence two photons produced after the η-decay. However the η meson can decay not only by the channel $\eta \to 2\gamma$ with the branching ratio BR=(39.38 ± 0.26)% but also by the channel $\eta \to 3\pi^0 \to 6\gamma$ with BR=(32.51 ± 0.28)%. The Monte Carlo simulation of the experiment shows that the most effective method of selecting events of the η-production process with the subsequent decay $\eta \to 2\gamma$ is to use the two-dimensional distribution in which the energy $E_{\gamma 1}$ deposited in one calorimeter is plotted *vs* the energy $E_{\gamma 2}$ deposited in another calorimeter. The result of such simulation is demonstrated in Fig. 7. A "banana"-shape spot clearly seen at photon energies from 200 to 400 MeV is due to photons from the decay $\eta \to 2\gamma$. On the base of such distribution cuts were chosen later on for the selection of "useful" events (*i. e.* events attributed to the η-production process with the subsequent decay $\eta \to 2\gamma$) – these cuts are shown in Fig. 7 as an ellipse within which 99% of the "useful" events are contained.

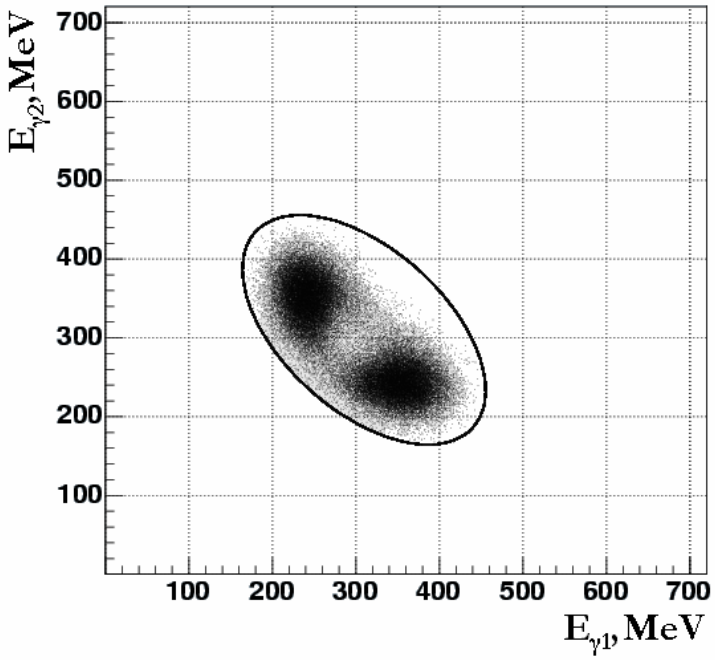

Fig. 7. Two-dimensional distribution $E_{\gamma 1}$ *vs* $E_{\gamma 2}$ obtained by the Monte Carlo simulation

Just such ellipse-shape cut was put after that on the similar two-dimensional distribution of real events obtained in the experiment. And all events inside this ellipse were considered to be "hydrogen" ones. Then the full angular range (from $\cos\theta_\eta^{cm} = -1$ to $\cos\theta_\eta^{cm} = +1$) was divided into 10 bins $\Delta\cos\theta_\eta^{cm} = 0.2$ and the differential cross sections for each bin were calculated using the formula similar (8).

The differential cross sections of the reaction $\pi^- p \to \eta n$ measured at the incident pions momenta of 700, 710, and 720 MeV/c are presented in Fig. 8. Shapes of the differential cross sections distinguish essentially

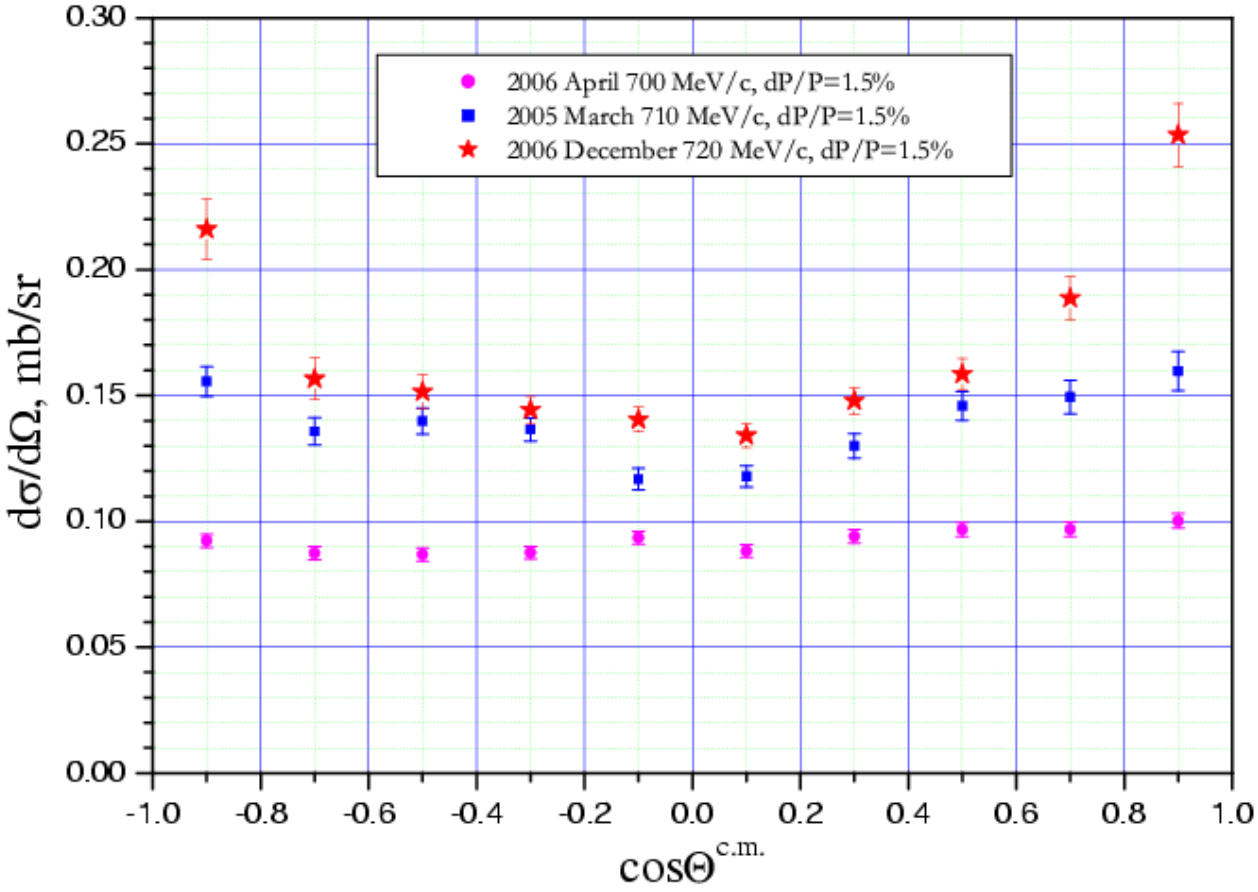

Fig. 8. Differential cross sections of the reaction $\pi^- p \to \eta n$ measured using the Neutral Meson Spectrometer

at different momenta – if at 700 MeV/c the angular dependence is practically flat, at 710 and 720 MeV/c it looks like a bowl profile. It may be considered as an evidence that at the momentum of 700 MeV/c only *S*-wave plays a role in the η-production process (*i.e.* this process goes through the formation of the $S_{11}(1535)$ resonance) but at higher momenta the contribution of *D*-wave became essential – it means that the η-production process goes partly through the formation of the $D_{13}(1520)$ resonance.

References

1. D.E. Bayadilov *et al.*, Preprint PNPI-2530, Gatchina, 2003. 20 p.
2. D.E. Bayadilov *et al.*, in *Proceedings of the 10th International Conference on Hadron Spectroscopy* (Aschaffenburg, Germany, 31 August – 6 September 2003), AIP Conference Proceedings **717**, 270 (2004).
3. D.E. Bayadilov *et al.*, Yad. Fiz. **67**, 512 (2004) [Phys. Atom. Nucl. **67**, 493 (2004)].
4. D.E. Bayadilov *et al.*, Preprint PNPI-2612, Gatchina, 2005. 34 p.
5. D.E. Bayadilov *et al.*, Preprint PNPI-2719, Gatchina, 2007. 13 p.